The Astrophysical Journal Letters, 726:L22 (6pp), 2011 January 10 doi:10.1088/2041-8205/726/2/L22

GREEN BANK TELESCOPE ZPECTROMETER CO(1–0) OBSERVATIONS OF THE STRONGLY LENSED SUBMILLIMETER GALAXIES FROM THE *HERSCHEL* ATLAS

D. T. Frayer[1], A. I. Harris[2], A. J. Baker[3], R. J. Ivison[4,5], Ian Smail[6], M. Negrello[7], R. Maddalena[1], I. Aretxaga[8], M. Baes[9], M. Birkinshaw[10], D. G. Bonfield[11], D. Burgarella[12], S. Buttiglione[13], A. Cava[14], D. L. Clements[15], A. Cooray[16], H. Dannerbauer[17], A. Dariush[18], G. De Zotti[13,19], J. S. Dunlop[20], L. Dunne[21], S. Dye[18], S. Eales[18], J. Fritz[9], J. Gonzalez-Nuevo[22], D. Herranz[23], R. Hopwood[7], D. H. Hughes[8], E. Ibar[4], M. J. Jarvis[11], G. Lagache[24], L. L. Leeuw[25,26], M. Lopez-Caniego[23], S. Maddox[21], M. J. Michałowski[20], A. Omont[27], M. Pohlen[18], E. Rigby[21], G. Rodighiero[28], D. Scott[29], S. Serjeant[7], D. J. B. Smith[21], A. M. Swinbank[6], P. Temi[30], M. A. Thompson[11], I. Valtchanov[31], P. P. van der Werf[5,32], and A. Verma[33]

[1] National Radio Astronomy Observatory, P.O. Box 2, Green Bank, WV 24944, USA
[2] Department of Astronomy, University of Maryland, College Park, MD 20742, USA
[3] Department of Physics and Astronomy, Rutgers, the State University of New Jersey, 136 Frelinghuysen Road, Piscataway, NJ 08854-8019, USA
[4] UK Astronomy Technology Centre, Royal Observatory, Blackford Hill, Edinburgh EH9 3HJ, UK
[5] Institute for Astronomy, University of Edinburgh, Royal Observatory, Blackford Hill, Edinburgh EH9 3HJ, UK
[6] Institute for Computational Cosmology, Physics Department, Durham University, South Road, Durham DH1 3LE, UK
[7] Department of Physics and Astronomy, The Open University, Milton Keynes MK7 6AA, UK
[8] Instituto Nacional de Astrofísica, Óptica y Electrónica Luis Enrique Erro, 1 Tonantzintla, Puebla 72840, Mexico
[9] Sterrenkundig Observatorium, Universiteit Gent, Krijgslaan 281 S9, B-9000 Gent, Belgium
[10] Department of Physics, University of Bristol, Tyndall Avenue, Bristol BS8 1TL, UK
[11] Centre for Astrophysics Research, Science & Technology Research Institute, University of Hertfordshire, Hatfield, Herts AL10 9AB, UK
[12] Laboratoire d'Astrophysique de Marseille, UMR6110 CNRS, 38 rue F. Joliot-Curie, 13388 Marseille, France
[13] INAF-Osservatorio Astronomico di Padova, Vicolo Osservatorio 5, I-35122 Padova, Italy
[14] Instituto de Astrofísica de Canarias, C/Vía Láctea s Laguna, Spain
[15] Physics Department, Imperial College London, Prince Consort Road, London SW7 2AZ, UK
[16] Center for Cosmology, University of California, Irvine, CA 92697, USA
[17] AIM, CEA/DSM-CNRS-Universit Paris Diderot, DAPNIA/Service d'Astrophysique, CEA Saclay, Orme De Merisiers, 91191 Gif-sur-Yvette Cedex, France
[18] School of Physics and Astronomy, Cardiff University, Cardiff CF24 3AA, UK
[19] SISSA, Via Bonomea 265, I-34136 Trieste, Italy
[20] Scottish Universities Physics Alliance, Institute for Astronomy, University of Edinburgh, Royal Observatory, Edinburgh EH9 3HJ, UK
[21] School of Physics and Astronomy, University of Nottingham, Nottingham NG7 2RD, UK
[22] Scuola Internazionale Superiore di Studi Avanzati, via Beirut 2-4, 34151 Triest, Italy
[23] Instituto de Fisica de Cantabria (CSIC-UC), Avda. los Castros s/n, 39005 Santander, Spain
[24] Institut d'Astrophysique Spatiale, Universit Paris-Sud 11 and CNRS (UMR 8617), F-91405 Orsay, France
[25] SETI Institute, 515 N. Whisman Avenue, Mountain View, CA 94043, USA
[26] Physics Department, University of Johannesburg, P.O. Box 524, Auckland Park 2006, South Africa
[27] Institut d'Astrophysique de Paris, CNRS and Université Pierre et Marie Curie, 98bis Bolulevard Arago, F-75014 Paris, France
[28] Department of Astronomy, University of Padova, Vicolo dell'Osservatorio 3, I-35122 Padova, Italy
[29] Department of Physics and Astronomy, University of British Columbia, Vancouver, BC V6T 1Z1, Canada
[30] Astrophysics Branch, NASA Ames Research Center, Mail Stop 245-6, Moffett Field, CA 94035, USA
[31] Herschel Science Centre, ESAC, ESA, P.O. Box 78, Villanueva de la Canada, 28691 Madrid, Spain
[32] Leiden Observatory, Leiden University, P.O. Box 9513, NL-2300 RA Leiden, The Netherlands
[33] Oxford Astrophysics, Denys Wilkinson Building, University of Oxford, Keble Road, Oxford OX1 3RH, UK
Received 2010 September 10; accepted 2010 November 19; published 2010 December 20

ABSTRACT

The *Herschel* Astrophysical Terahertz Large Area Survey (H-ATLAS) has uncovered a population of strongly lensed submillimeter galaxies (SMGs). The Zpectrometer instrument on the Green Bank Telescope (GBT) was used to measure the redshifts and constrain the masses of the cold molecular gas reservoirs for two candidate high-redshift lensed sources. We derive CO(1–0) redshifts of $z = 3.042 \pm 0.001$ and $z = 2.625 \pm 0.001$, and measure molecular gas masses of (1–3) $\times 10^{10}\,M_{\odot}$, corrected for lens amplification and assuming a conversion factor of $\alpha = 0.8\,M_{\odot}\,(\mathrm{K\,km\,s^{-1}\,pc^{2}})^{-1}$. We find typical $L(\mathrm{IR})/L'(\mathrm{CO})$ ratios of 120 ± 40 and $140 \pm 50\,L_{\odot}\,(\mathrm{K\,km\,s^{-1}\,pc^{2}})^{-1}$, which are consistent with those found for local ultraluminous infrared galaxies (ULIRGs) and other high-redshift SMGs. From analysis of published data, we find no evidence for enhanced $L(\mathrm{IR})/L'(\mathrm{CO}(1\text{–}0))$ ratios for the SMG population in comparison to local ULIRGs. The GBT results highlight the power of using the CO lines to derive blind redshifts, which is challenging for the SMGs at optical wavelengths given their high obscuration.

Key words: galaxies: evolution – galaxies: formation – galaxies: individual (SDP.81: H-ATLAS J090311.6+003906, SDP.130: H-ATLAS J091305.0−005343) – galaxies: starburst

1. INTRODUCTION

The discovery of the submillimeter galaxies (SMGs) 13 years ago revolutionized our understanding of galaxy formation and evolution by uncovering a population of high-redshift, dust-obscured systems that are forming stars at tremendous rates (Smail et al. 1997). In terms of their infrared luminosities, the SMGs are analogous to the local ultraluminous infrared galaxies (ULIRGs). Until recently, deep observations at far-infrared (FIR)/submillimeter wavelengths have been either limited to relatively small areas of the sky or severely affected by source confusion due to poor spatial resolution. The

Herschel Space Observatory (Pilbratt et al. 2010) has enormously extended the sky coverage at FIR/submillimeter wavelengths. The *Herschel* Astrophysical Terahertz Large Area Survey (H-ATLAS; Eales et al. 2010) will map 570 deg^2 in five bands from 100 to 500 μm. As pointed out by Blain (1996), the submillimeter band is well suited for generating large samples of strongly lensed galaxies at high redshift due to the large negative k-correction and steep source counts. The Science Demonstration Phase (SDP) H-ATLAS observations have confirmed the excess of bright lensed SMGs over the expected number counts of unlensed galaxies (Negrello et al. 2010), which is consistent with the results found from the South Pole Telescope Survey (Vieira et al. 2010; Lima et al. 2010).

Deriving redshifts for the lensed SMGs is challenging using traditional optical and near-infrared techniques. The SMGs themselves are highly obscured, and the foreground lensing galaxies dominate the emission seen at optical and near-infrared wavelengths. However, we are no longer limited to these traditional techniques. The new generation of wide bandwidth spectrometers operating at centimeter/millimeter/submillimeter wavelengths now make it possible to determine redshifts directly from the CO rotational lines (e.g., Weiß et al. 2009; Swinbank et al. 2010). In addition to accurate redshift measurements, CO observations are fundamental to our understanding of galaxy evolution by measuring the mass of the molecular gas reservoir from which stars form. The first two SMGs in which CO was detected (Frayer et al. 1998, 1999) were relatively bright at optical wavelengths, which enabled timely follow-up CO observations. Subsequent CO detections of additional SMGs took several years. In general, deep radio or millimeter/submillimeter wavelength interferometric continuum maps were required to derive accurate counterpart positions (Frayer et al. 2000; Ivison et al. 2002; Dannerbauer et al. 2002; Younger et al. 2009). Then, deep spectroscopic observations were necessary to obtain redshifts (Ivison et al. 1998; Barger et al. 1999; Frayer et al. 2003; Chapman et al. 2005). With accurate redshifts, CO observations were finally possible (e.g., Neri et al. 2003; Greve et al. 2005). Hence, the process of following-up SMGs in CO used to be very time consuming. Now, using the wide bandwidth radio spectrometers, we can bypass the intermediate steps and directly search for CO lines at the location of the SMGs uncovered by *Herschel* and other submillimeter instruments. An additional important advantage of direct CO searches is that we avoid the biases related to the radio and optical selection of candidate SMG counterparts.

In this Letter, we report on CO(1–0) observations of two lensed SMGs (SDP.81 and SDP.130) uncovered by the H-ATLAS program using the wide bandwidth Zpectrometer instrument on the Robert C. Byrd Green Bank Telescope (GBT) operated by the National Radio Astronomy Observatory (NRAO). A cosmology of $H_0 = 70\,\mathrm{km\,s^{-1}\,Mpc^{-1}}$, $\Omega_\mathrm{M} = 0.3$, and $\Omega_\Lambda = 0.7$ is assumed throughout this Letter.

2. OBSERVATIONS

The discovery of the lensed SMGs SDP.81 (H-ATLAS J090311.6+003906) and SDP.130 (H-ATLAS J091305.0−005343) was reported by Negrello et al. (2010). Both of these sources have spectral energy distributions (SEDs) that peak in the 350 μm band, suggesting redshifts of $z \sim 2.5$–3 assuming local ULIRG SEDs that peak at 80–100 μm in their rest frame. Given their strong observed-frame 350 μm emission (180 mJy and 130 mJy for SDP.81 and SDP.130, respectively), they were ideal targets for the Zpectrometer instrument on the GBT. The instrument currently covers the 25.61–36.09 GHz band corresponding to redshifted CO(1–0) from $z = 2.19$ to $z = 3.50$. The Zpectrometer is an analog lag cross-correlator spectrometer connected to the GBT dual-channel K_a-band correlation receiver (see Harris et al. 2010 for additional details).

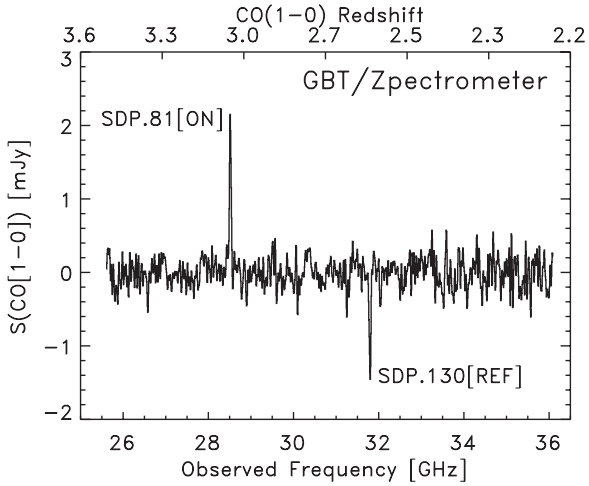

Figure 1. Full GBT/Zpectrometer difference spectrum for SDP.81 (ON source) and SDP.130 (REF source) showing the detections of CO(1–0) emission for both. SDP.81 was detected at the 12σ level, while SDP.130 was detected at 7σ (Table 1).

The Zpectrometer observations of SDP.81 and SDP.130 were carried out on 2010 March 24 and April 21 (GBT program 10A-77). The observations were taken using the sub-reflector beam switching ("SubBeamNod") mode with a 10 s switching interval. Alternating sets of SubBeamNod observations between the two targets were taken every 4 minutes to remove the residual baseline structure. By differencing the resulting spectra of the two targets SDP.81 ("ON" position) and SDP.130 ("REF" position) flat baselines were achieved (Figure 1). We obtained 2.3 hr of effective integration time (1.15 hr of ON time and 1.15 hr of REF time). During the observing cycle, the observations were about 65% efficient. Including the additional time for pointing, focus, and calibration, 5.5 hr of telescope time were used. Spectra of the pointing source 0825+0309 were taken every hour to monitor gain variations. The absolute flux density scale was derived from observations of 3C286. We adopt a flux density of 2.04 Jy at 32 GHz for 3C286 (Ott et al. 1994). After correcting for atmospheric opacity effects and based on the dispersion of measurements observed for 0825+0309, we estimate a 15% absolute calibration uncertainty for the data.

3. RESULTS

We observe strong emission lines in the spectra of both SDP.81 and SDP.130 which we identify as CO(1–0), yielding redshifts of $z = 3.042$ and $z = 2.625$, respectively (Figure 1). Follow-up CO(3–2) observations made with the Plateau de Bure Interferometer (PdBI; R. Neri et al. 2011, in preparation), and the higher-level CO transitions observed with the Caltech Submillimeter Observatory (CSO) Z-Spec instrument (Lupu et al. 2010) confirm the CO(1–0) line identifications with the GBT. Single-component Gaussian fits to the lines were made to derive the CO(1–0) properties (Table 1). The CO(1–0) profiles are slightly asymmetric in directions consistent with the PdBI CO(3–2) profiles, but given the limited CO(1–0) spectral resolution, the Zpectrometer profiles are consistent

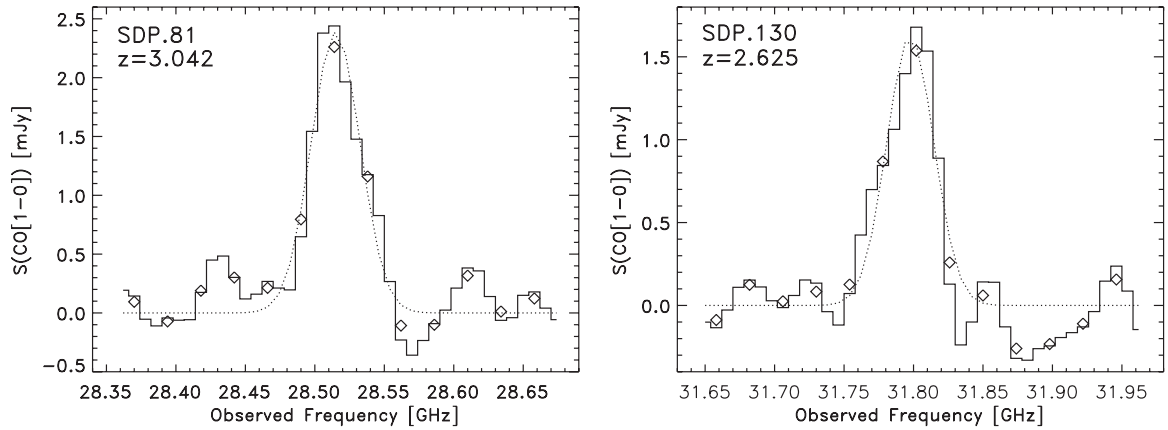

Figure 2. CO(1–0) spectra for SDP.81 (left) and SDP.130 (right). The solid-line histograms show the raw data, and the Gaussian fits to the raw data are shown by the dotted lines. The diamonds represent independent 24 MHz channels derived by binning the raw data by three channels.

Table 1
CO(1–0) Observational Results

Parameter	SDP.81	SDP.130
Line peak S_ν (mJy)	2.39 ± 0.19	1.63 ± 0.22
FWHM ΔV (km s^{-1})	435 ± 54	377 ± 62
Integrated line flux S(CO) (Jy km s^{-1})[a]	1.11 ± 0.25	0.65 ± 0.19
Line center (topocentric) (GHz)	28.515 ± 0.003	31.798 ± 0.005
Redshift (z(LSR))	3.042 ± 0.001	2.625 ± 0.001
L(CO) (10^6 $L_\odot$][b]	0.9 ± 0.3	1.7 ± 0.5
L'(CO) (10^{10} K km s^{-1} pc^2)[b]	1.8 ± 0.7	3.4 ± 1.0
M(H$_2$) ($M_\odot$)[b,c]	$\sim 1.4 \times 10^{10}$	$\sim 2.7 \times 10^{10}$
L(IR) (10^{12} $L_\odot$)[b,d]	2.1 ± 0.7	4.7 ± 1.3
L(IR)/L'(CO(1–0)) ($L_\odot$ (K km s^{-1} pc^2)$^{-1}$)[e]	120 ± 40	140 ± 50

Notes.
[a] Uncertainty on the total CO(1–0) line flux includes the 15% systematic calibration uncertainty added to the statistical noise of the line.
[b] Corrected for the lensing amplification factors of 25 ± 7 for SDP.81 and 6 ± 1 for SDP.130 (Negrello et al. 2010).
[c] Adopting $\alpha = 0.8\,M_\odot$ (K km s^{-1} pc^2)$^{-1}$ (Downes & Solomon 1998) which could be uncertain by a factor of two or more.
[d] L(IR)(8–1000 μm) based on fitting an Arp 220 template.
[e] Assuming no differential lensing between the CO and infrared emission.

with a single Gaussian. The instrumental spectral response is nearly a sinc function with a full width at half-maximum (FWHM) of 20 MHz. For intrinsic Gaussian FWHM line widths larger than 30 MHz (∼300 km s^{-1}), the line width correction for the instrumental response is less than 1%. Figure 2 shows the Gaussian fits to the raw 8 MHz channels. The raw channels were binned by three channels to yield statistically independent channels. We achieved an rms of 0.18 mJy per 24 MHz channel, albeit with significant variation across the full Zpectrometer bandwidth. The observations were taken at fixed frequencies (topocentric velocity scale). Small Doppler corrections of 35 km s^{-1} were applied to the observed line centers to derive the redshifts with respect to the local standard of rest (LSR, Table 1).

The mass of molecular gas (including He) is computed using $M(\mathrm{H_2})/L'(\mathrm{CO(1–0)}) = \alpha$, where the CO(1–0) line luminosity is in units of K km s^{-1} pc^2 (Solomon et al. 1997). While there is still considerable discussion about the appropriate value for α at high redshift (e.g., Tacconi et al. 2008; Ivison et al. 2010a), we adopt the "standard" local ULIRG value of $\alpha = 0.8\,M_\odot$ (K km s^{-1} pc^2)$^{-1}$ (Downes & Solomon 1998) for direct comparison with previous studies. However, a higher value may be more appropriate for the expected multi-phase molecular interstellar medium (ISM) in strong starburst systems (Papadopoulos et al. 2007; Harris et al. 2010; Danielson et al. 2010; Ivison et al. 2010a).

4. DISCUSSION

4.1. CO Properties

Observations of CO(1–0) are key for deriving the total molecular gas mass. The CO(1–0) line traces the cold material not probed by the higher-level CO transitions. Unfortunately, most high-redshift sources to date have been observed in only the higher-level $J_{\rm upper} > 1$ transitions (e.g., CO(3–2) or higher), and many papers have assumed a single-component ISM that is fully thermalized with $T_b(J_{\rm upper} > 1)/T_b(1-0) = L'(J_{\rm upper} > 1)/L'(\mathrm{CO(1–0)}) = 1$. However, recent CO(1–0) observations of the SMG population show that this assumption is not correct (Harris et al. 2010; Carilli et al. 2010; Swinbank et al. 2010; Ivison et al. 2010a, 2010b). From the compilation of these previous results, an average CO line ratio value of $r_{31} = L'(\mathrm{CO(3–2)})/L'(\mathrm{CO(1–0)}) = 0.6 \pm 0.1$ is found for a

sample of nine SMGs. SDP.81 and SDP.130 also have ratios of less than unity. Based on the CO(3–2) observations made with the PdBI (R. Neri et al. 2011, in preparation), SDP.81 and SDP.130 have r_{31} ratios of 0.5 and 0.7, respectively. These ratios are in agreement with the previous SMG results as well as the average value of $r_{31} \simeq 0.6$ measured for local infrared galaxies (Yao et al. 2003; Leech et al. 2010). Although the values measured for SMGs are similar to the average value found for the local starburst population, there are significant variations in the ratio locally ($r_{31} = 0.1$–1). The possible wide range of CO line ratios highlights the importance of obtaining CO(1–0) observations for the SMGs and other high-redshift populations for comparison. For example, the BzK galaxies may show similar "sub-thermal" CO line ratios as the SMGs (Dannerbauer et al. 2009; Aravena et al. 2010), while in contrast high-redshift quasars tend to show CO lines ratios of order unity up to CO(4–3) or even higher transitions (e.g., Riechers et al. 2006).

Based on their L'(CO(1–0)) luminosities corrected for amplification by lensing (Table 1), the derived molecular gas masses for SDP.81 and SDP.130 are (1–3)$\times 10^{10}\ M_{\odot}$, which is about 3–5 times larger than that found for local ULIRGs (Downes & Solomon 1998), but is consistent with other SMGs studied to date (adopting the same $\alpha = 0.8\ M_{\odot}\ (\mathrm{K\,km\,s^{-1}\,pc^2})^{-1}$). Since the infrared luminosity is proportional to the star formation rate and the CO luminosity is proportional to the molecular gas mass, the infrared-to-CO luminosity ratio provides an indication of the star formation efficiency. However, given the uncertainties of converting the observables into physical quantities (especially the uncertainty of α), we restrict the discussion to the observed $L(\mathrm{IR})/L'(\mathrm{CO(1–0)})$ ratios. Strong starbursts and ULIRGs tend to show high IR-to-CO luminosity ratios of $\gtrsim 100\ L_{\odot}\ (\mathrm{K\,km\,s^{-1}\,pc^2})^{-1}$, while local spiral galaxies have lower values of about 10–50 (e.g., Solomon & Vanden Bout 2005). Based on their infrared luminosities (Table 1), SDP.81 and SDP.130 have $L(\mathrm{IR})/L'(\mathrm{CO(1–0)})$ ratios of 120 and 140 $L_{\odot}\ (\mathrm{K\,km\,s^{-1}\,pc^2})^{-1}$, respectively.

Greve et al. (2005) found an average $L(\mathrm{IR})/L'(\mathrm{CO})$ ratio for SMGs which was a factor of two larger than that for local ULIRGs. However, if the published data are corrected for the same cosmology (Section 1), infrared luminosity definition (L(IR), 8–1000 μm), and for the same CO(1–0) transition, the SMGs actually show a slightly lower $L(\mathrm{IR})/L'(\mathrm{CO(1–0)})$ ratio on average in comparison to local ULIRGs. We recomputed the infrared luminosities for the local ULIRG sample given by Solomon et al. (1997), using the relationship in Sanders & Mirabel (1996) and find a median value of $L(\mathrm{IR})/L'(\mathrm{CO(1–0)}) = (240 \pm 60)\ L_{\odot}\ (\mathrm{K\,km\,s^{-1}\,pc^2})^{-1}$ (for $L(\mathrm{IR}) > 10^{12}\ L_{\odot}$). The uncertainty represents the standard deviation of the ratio for the sample after throwing out one outlier, divided by the square root of the number of sources (28), and includes an additional 15% systematic calibration uncertainty. Adopting $r_{31} = 0.6$, the implied L'(CO(1–0)) values for SMGs are increased by a factor of 1.67 in comparison to Greve et al. (2005) which assumed $r_{31} = 1$. The average L(IR) value from Greve et al. (2005) also needs to be decreased by roughly a factor of two due to the lower observed dust temperatures measured for the SMGs (Kovács et al. 2006; Magnelli et al. 2010). After making these corrections, the Greve et al. (2005) results suggest an average value of $L(\mathrm{IR})/L'(\mathrm{CO(1–0)}) = 110 \pm 40\ L_{\odot}\ (\mathrm{K\,km\,s^{-1}\,pc^2})^{-1}$ for the SMG population. This value is consistent with those found for SDP.81 and SDP.130 and suggests that SMGs do not have enhanced $L(\mathrm{IR})/L'(\mathrm{CO(1–0)})$ ratios in comparison to local ULIRGs.

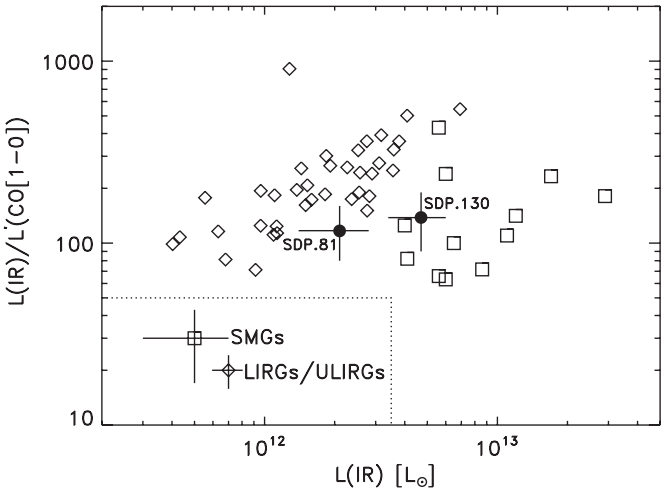

Figure 3. $L(\mathrm{IR})/L'(\mathrm{CO(1–0)})$ luminosity ratio in units of $L_{\odot}\ (\mathrm{K\,km\,s^{-1}\,pc^2})^{-1}$ for local LIRGs/ULIRGs given by Solomon et al. (1997; diamonds) and a sample of SMGs (squares; Greve et al. 2003, 2005; Kovács et al. 2006; Solomon & Vanden Bout 2005; Frayer et al. 2008; Daddi et al. 2009; Carilli et al. 2010; Ivison et al. 2010b; Coppin et al. 2010; Riechers et al. 2010). All SMGs were chosen based on the existence of infrared measurements near the peak of their rest-frame SED (60–180 μm). Based on the CO line ratios found for the SMGs and ULIRGs, the published data were converted to CO(1–0) luminosities adopting $r_{21} = 0.8$, $r_{31} = 0.6$, and $r_{41} = 0.4$ for the SMGs without CO(1–0) detections. All points assume the same cosmology and infrared luminosity definition (8–1000 μm). The SMGs SDP.81 and SDP.130 are shown by the solid points, and the approximate errors for the other points are given by the crosses at the lower left.

We carried out an additional comparison with the local ULIRGs, by using only SMGs with infrared measurements near the peak of their rest-frame SED (60–180 μm, Figure 3). This improves the derivations of L(IR) that are dependent on the assumed SED template. Including SDP.81 and SDP.130 with a sample of published SMGs (Figure 3), we derive a median value of $L(\mathrm{IR})/L'(\mathrm{CO(1–0)}) = 125 \pm 50\ L_{\odot}\ (\mathrm{K\,km\,s^{-1}\,pc^2})^{-1}$ for the SMG population. For sources without CO(1–0) detections, the published data were converted to CO(1–0) luminosities adopting $r_{21} = L'[\mathrm{CO(2–1)}]/L'[\mathrm{CO(1–0)}] = 0.8 \pm 0.1$, $r_{31} = L'[\mathrm{CO(3–2)}]/L'[\mathrm{CO(1–0)}] = 0.6 \pm 0.1$, and $r_{41} = L'[\mathrm{CO(4–3)}]/L'[\mathrm{CO(1–0)}] = 0.4 \pm 0.1$. The adopted r_{41} and r_{21} values are consistent with simple large-velocity gradient excitation analysis based on $r_{31} = 0.6$ (with temperatures of 20–50 K and molecular gas densities of order 1000 cm^{-3}) and are consistent with current observations of local luminous starbursts.

A direct comparison of the $L(\mathrm{IR})/L'(\mathrm{CO(1–0)})$ ratios with that of local ULIRGs is complicated by the possibility of strong mid-infrared emission (rest frame 25 μm). The SMG templates used to derive L(IR) do not include possible excess mid-infrared emission, which is present in some local ULIRGs. However, if we neglect the mid-infrared emission for local ULIRGs, the median $L(\mathrm{IR})/L'(\mathrm{CO(1–0)})$ ratio would decrease by only 10%. Including this small possible correction for mid-infrared emission, the median $L(\mathrm{IR})/L'(\mathrm{CO(1–0)})$ value for SMGs is 0.6 ± 0.3 times that found for local ULIRGs, i.e., the median ratio is slightly lower in SMGs, but roughly consistent with local ULIRGs within uncertainties.

The observed r_{31} brightness temperature ratios and the $L(\mathrm{IR})/L'(\mathrm{CO})$ luminosity ratios for SDP.81 and SDP.130 are similar to values found for ULIRGs and other SMGs. Since the CO(1–0) emission traces the cold gas, which is typically

Table 2
Instruments for CO Redshift Searches

Telescope	Instrument	Frequency Range	Bandwidth	Sensitivity (5σ)[a]
GBT	Zpectrometer	25.6–36.1 GHz	34%	0.9 mJy (This work)
CSO	Z-Spec	190–305 GHz	46%	100 mJy (Lupu et al. 2010)
CSO	ZEUS[b]	632–710 GHz	4%	300 mJy (Ferkinhoff et al. 2010)
IRAM 30 m	EMIR[b]	83–117 GHz	8%	9 mJy (IRAM documentation)
PdBI	WideX[b]	80–116 GHz	3.6%	3.7 mJy (Daddi et al. 2009)
CARMA[b,c]		85–116 GHz	8%	13 mJy (Web calculator)
EVLA[c]	WIDAR	12–50 GHz	40%–18%	0.2–0.4 mJy (Project page)
LMT[d]	RSR	74–111 GHz	40%	4 mJy (32 m), 1.5 mJy (50 m)[e]
ALMA[b,d]		84–116 GHz	8%	0.4 mJy (Web calculator)

Notes.
[a] Estimated 5σ sensitivity with 1 hr of on source integration for a line width of 300 km s^{-1}. Please consult observatory documentation for updated estimates of sensitivity.
[b] Higher frequency bands with lower fractional bandwidth also available.
[c] The Combined Array for Research in Millimeter Astronomy (CARMA) has a mixture of 4 GHz and 8 GHz bandwidths.
[d] System still in development.
[e] The LMT sensitivity estimated for the initial 32 m telescope and the final 50 m telescope.

more spatially extended than the CO(3–2) emission (Ivison et al. 2010a), differential lensing could impact the interpretation of the results for SDP.81 and SDP.130. If differential lensing is important, then the intrinsic r_{31} ratios for SDP.81 and SDP.130 may be even lower than the values derived here.

4.2. CO Redshift Surveys

The new generation of broad bandwidth spectrometers now enables blind redshift searches for CO emission (see conference proceedings of Baker et al. 2007). The first blind redshift for the Zpectrometer instrument was found for SMM J2135-0102 (Swinbank et al. 2010). SDP.81 and SDP.130 represent additional blind redshifts from the Zpectrometer. The first blind CO redshift for the CSO Z-Spec instrument was found for SDP.81 (Lupu et al. 2010). Weiß et al. (2009) reported the first blind CO redshift using the Institut de Radioastronomie Millimétrique (IRAM) 30 m Eight MIxer Receiver (EMIR) instrument, and Daddi et al. (2009) and M. Krips et al. (2011, in preparation) have successfully used the PdBI to uncover previously unknown redshifts with CO lines. Table 2 shows the capabilities of the current and planned instrumentation for CO redshift machines. Based on the combination of its large fractional bandwidth (34%) and good sensitivity, the GBT/Zpectrometer is currently the most efficient system for searching for CO(1–0) lines at redshifts $2.2 < z < 3.5$. Although not as sensitive as the GBT, the Z-Spec instrument has a larger fractional bandwidth (46%) and can search all redshifts using a variety of transitions. At the highest frequencies, CO searches may be difficult due to subthermal excitation of the high-J CO lines, and the atomic lines such as [C I] and [C II] may be more feasible (e.g., Wagg et al. 2010). A primary science driver for the Large Millimeter Telescope (LMT) is CO redshift searches at 3 mm using the Redshift Search Receiver (RSR; Erickson et al. 2007). When the Expanded Very Large Array (EVLA) achieves its full 8 GHz of bandwidth, it will be able to search for CO(1–0) at redshifts $z > 1.3$ with better sensitivity than that of the GBT/Zpectrometer (Table 2).

5. CONCLUDING REMARKS

The SMGs SDP.81 and SDP.130 are two of the first examples of the lensed SMG population discovered by the *Herschel Space Observatory* (Negrello et al. 2010). They have CO properties similar to those found for other high-redshift SMGs and local ULIRGs in terms of their CO line ratios and their infrared-to-CO luminosity ratios. In contrast to previous results, we find no evidence for enhanced $L(\mathrm{IR})/L'(\mathrm{CO})$ ratios for the SMGs in comparison to local ULIRGs. Given their high amplification, the *Herschel* population of lensed SMGs provides ideal targets for studying the ISM properties at high redshift, by allowing observations of fainter lines, such as HCN, ^{13}CO, and [C I], which would otherwise be too faint. Studying multiple molecular species and detailed imaging of several CO transitions are required to constrain the different components of the molecular ISM at high redshift and their CO to H_2 conversion factors.

In the upcoming era of high-resolution imaging with the Atacama Large Millimeter/submillimeter Array (ALMA) and the EVLA, large single dishes will still have a major role to play in spectroscopic CO surveys. The GBT, LMT, and eventually the Cerro Chajnantor Atacama Telescope will be able to determine redshifts for significant samples of highly obscured SMGs which are not measurable with even the largest optical and near-infrared telescopes.

We acknowledge the staff at Green Bank who have made these observations possible. We are indebted to the late Senator Robert C. Byrd for his strong support of the Green Bank Telescope. The National Radio Astronomy Observatory is a facility of the National Science Foundation operated under cooperative agreement by Associated Universities, Inc. A.J.B. acknowledges support from the National Science Foundation through grant AST-0708653.

Facility: GBT (Zpectrometer)

REFERENCES

Aravena, M., et al. 2010, ApJ, 718, 177
Baker, A. J., Glenn, J., Harris, A. I., Mangum, J. G., & Yun, M. S. (ed.) 2007, ASP Conf. Ser. 375, From Z-Machines to ALMA: (Sub)Millimeter Spectroscopy of Galaxies (San Francisco, CA: ASP)
Barger, A. J., Cowie, L. L., Smail, I., Ivison, R. J., Blain, A. W., & Kneib, J.-P. 1999, AJ, 117, 2656
Blain, A. W. 1996, MNRAS, 283, 1340
Carilli, C. L., et al. 2010, ApJ, 714, 1407
Chapman, S. C., Blain, A. W., Smail, I., & Ivison, R. J. 2005, ApJ, 622, 772
Coppin, K. E. K., et al. 2010, MNRAS, 407, L103

Daddi, E., Dannerbauer, H., Krips, M., Walter, F., Dickinson, M., Elbaz, D., & Morrison, G. E. 2009, ApJ, 695, L176
Danielson, A. L. R., et al. 2010, MNRAS, in press (arXiv:1008.3183)
Dannerbauer, H., Daddi, E., Riechers, D. A., Walter, F., Carilli, C. L., Dickinson, M., Elbaz, D., & Morrison, G. E. 2009, ApJ, 698, L178
Dannerbauer, H., et al. 2002, ApJ, 573, 473
Downes, D., & Solomon, P. M. 1998, ApJ, 507, 615
Eales, S., et al. 2010, PASP, 122, 499
Erickson, N., Narayanan, G., Goeller, R., & Grosslein, R. 2007, in ASP Conf. Ser. 375, From Z-Machines to ALMA: (Sub)Millimeter Spectroscopy of Galaxies, ed. A. J. Baker et al. (San Francisco, CA: ASP), 71
Ferkinhoff, C., Hailey-Dunsheath, S., Nikola, T., Parshley, S. C., Stacey, G. J., Benford, D. J., & Staguhn, J. G. 2010, ApJ, 714, L147
Frayer, D. T., Armus, L., Scoville, N. Z., Blain, A. W., Reddy, N. A., Ivison, R. J., & Smail, I. 2003, AJ, 126, 73
Frayer, D. T., Ivison, R. J., Scoville, N. Z., Yun, M., Evans, A. S., Smail, I., Blain, A. W., & Kneib, J.-P. 1998, ApJ, 506, L7
Frayer, D. T., Smail, I., Ivison, R. J., & Scoville, N. Z. 2000, AJ, 120, 1668
Frayer, D. T., et al. 1999, ApJ, 514, L13
Frayer, D. T., et al. 2008, ApJ, 680, L21
Greve, T. R., Ivison, R. J., & Papadopoulos, P. P. 2003, ApJ, 599, 839
Greve, T. R., et al. 2005, MNRAS, 359, 1165
Harris, A. I., Baker, A. J., Zonak, S. G., Sharon, C. E., Genzel, R., Rauch, K., Watts, G., & Creager, R. 2010, ApJ, 723, 1139
Ivison, R. J., Papadopoulos, P. P., Smail, I., Greve, T. R., Thomson, A. P., Xilouris, E. M., & Chapman, S. C. 2010a, MNRAS, submitted (arXiv:1009.0749)
Ivison, R. J., Smail, I., Le Borgne, J.-F., Blain, A. W., Kneib, J.-P., Bezecourt, J., Kerr, T. H., & Davies, J. K. 1998, MNRAS, 298, 583
Ivison, R. J., Smail, I., Papadopoulos, P. P., Wold, I., Richard, J., Swinbank, A. M., Kneib, J.-P., & Owen, F. N. 2010b, MNRAS, 404, 198
Ivison, R. J., et al. 2002, MNRAS, 337, 1
Kovács, A., Chapman, S. C., Dowell, C. D., Blain, A. W., Ivison, R. J., Smail, I., & Phillips, T. G. 2006, ApJ, 650, 592
Leech, J., Isaak, K. G., Papadopoulos, P. P., Gao, Y., & Davis, G. R. 2010, MNRAS, 406, 1364
Lima, M., Jain, B., Devlin, M., & Aguirre, J. 2010, ApJ, 717, L31
Lupu, R. E., et al. 2010, ApJ, submitted (arXiv:1009.5983)
Magnelli, B., et al. 2010, A&A, 518, L28
Negrello, M., et al. 2010, Science, 330, 800
Neri, R., et al. 2003, ApJ, 597, L113
Ott, M., Witzel, A., Quirrenbach, A., Krichbaum, T. P., Standke, K. J., Schalinski, C. J., & Hummel, C. A. 1994, A&A, 284, 331
Papadopoulos, P. P., Isaak, K. G., & van der Werf, P. P. 2007, ApJ, 668, 815
Pilbratt, G. L., et al. 2010, A&A, 518, L1
Riechers, D. A., et al. 2006, ApJ, 650, 604
Riechers, D. A., et al. 2010, ApJ, 720, L131
Sanders, D. B., & Mirabel, I. F. 1996, ARA&A, 34, 749
Smail, I., Ivison, R. J., & Blain, A. W. 1997, ApJ, 490, L5
Solomon, P. M., Downes, D., Radford, S. J. E., & Barrett, J. W. 1997, ApJ, 478, 144
Solomon, P. M., & Vanden Bout, P. A. 2005, ARA&A, 43, 677
Swinbank, A. M., et al. 2010, Nature, 464, 733
Tacconi, L. J., et al. 2008, ApJ, 680, 246
Vieira, J. D., et al. 2010, ApJ, 719, 763
Wagg, J., Carilli, C. L., Wilner, D. J., Cox, P., De Breuck, C., Menten, K., Riechers, D. A., & Walter, F. 2010, A&A, 519, L1
Weiß, A., Ivison, R. J., Downes, D., Walter, F., Cirasuolo, M., & Menten, K. M. 2009, ApJ, 705, L45
Yao, L., Seaquist, E. R., Kuno, N., & Dunne, L. 2003, ApJ, 588, 771
Younger, J. D., et al. 2009, ApJ, 704, 803